Transgenic expression of human glial cell line-derived neurotrophic factor (*hGDNF*) from integration-deficient lentiviral vectors is neuroprotective in a rodent model of Parkinson's disease

Ngoc B. Lu-Nguyen[1], Martin Broadstock[1†], Maximilian G. Schliesser[1,2], Cynthia C. Bartholomae[2], Christof von Kalle[2], Manfred Schmidt[2] and Rafael J. Yáñez-Muñoz[1,*]

Author Affiliations:

[1]School of Biological Sciences, Royal Holloway University of London, Egham, Surrey, TW20 0EX, UK.

[2]National Center for Tumor Diseases, Department of Translational Oncology, German Cancer Research Center, Im Neuenheimer Feld 350, 69120 Heidelberg, Germany

[†]Current address: King's College London, Wolfson Centre for Age-Related Diseases, Guy's Campus, London SE1 1UL, UK.

***Corresponding author:** Dr Rafael J. Yáñez-Muñoz, School of Biological Sciences, Royal Holloway University of London, Egham, Surrey, TW20 0EX, UK.

Tel: +44 (0) 1784 443180, Fax: +44 (0) 1784 414224, Email: rafael.yanez@rhul.ac.uk

Short title: Episomal lentivectors neuroprotect in Parkinson's.

Abstract

Standard integration-proficient lentiviral vectors (IPLVs) are effective at much lower doses than other vector systems and have shown promise for gene therapy of Parkinson's disease. Their main drawback is the risk of insertional mutagenesis. The novel biosafety-enhanced integration-deficient lentiviral vectors (IDLVs) may offer a significant enhancement in bio-safety, but have not been previously tested in a model of a major disease. We have assessed bio-safety and transduction efficiency of IDLVs in a rat model of Parkinson's disease, using IPLVs as a reference. Genomic insertion of lentivectors injected into the lesioned striatum was studied by linear amplification-mediated PCR, followed by deep sequencing and insertion site analysis, demonstrating lack of significant IDLV integration. Reporter gene expression studies showed efficient, long-lived and transcriptionally targeted expression from IDLVs injected ahead of lesioning in the rat striatum, albeit at somewhat lower expression levels than from IPLVs. Transgenic human glial cell line-derived neurotrophic factor (*hGDNF*) expression from IDLVs was used for a long-term investigation of lentivector-mediated, transcriptionally targeted neuroprotection in this Parkinson's disease rat model. Vectors were injected before striatal lesioning and the results showed improvements in nigral dopaminergic neuron survival and behavioral tests regardless of lentiviral integration proficiency, although they confirmed lower expression levels of *hGDNF* from IDLVs. These data demonstrate the effectiveness of IDLVs in a model of a major disease and indicate that these vectors could provide long-term Parkinson's disease treatment at low dose, combining efficacy and bio-safety for targeted central nervous system applications.

Introduction

Lentiviral vectors and adeno-associated viral vectors (AAVs) have been widely used for pre-clinical and some clinical gene therapies in the central nervous system (CNS) (Abordo-Adesida and others 2005; Bjorklund and others 2000). Retroviral vector integration has mediated some serious adverse events in clinical trials (Hacein-Bey-Abina and others 2003) and although lentiviral vectors have a safer profile (Aiuti and others 2013; Biffi and others 2011), some examples of feline lentiviral vector-mediated oncogenesis have been reported in foetal models (Condiotti and others 2013; Nowrouzi and others 2013; Themis and others 2005). In contrast, integration-deficient lentiviral vectors (IDLVs) have provided similar transduction efficiencies to classical integration-proficient lentiviral vectors (IPLVs) in a range of cell types, whilst having a significantly reduced risk of insertional mutagenesis (Wanisch and Yáñez-Muñoz 2009; Yáñez-Muñoz and others 2006). IDLVs are commonly produced using class I integrase mutations (most frequently encoding a D64V change), whereby viral DNA fails to integrate into the host genome and forms episomal DNA circles instead. As these viral episomes lack replication signals, they are stable in quiescent cells but progressively diluted in proliferating cells. Hence, IDLVs are ideally suited for applications in the post-mitotic CNS environment (Peluffo and others 2013), but to our knowledge they have not been previously applied in the study of a major disease. Additionally, most experiments using IDLVs have focused on a relatively short time scale (weeks), with very few studies so far confirming efficient and long-lasting CNS gene expression *in vivo* (Apolonia and others 2007; Hutson and others 2012; Philippe and others 2006; Rahim and others 2009; Yáñez-Muñoz and others 2006).

Parkinson's disease (PD) affects over 6 million individuals worldwide and is considered the second most common neurodegenerative disease, after Alzheimer's disease (Lyons and Pahwa 2011). PD is an idiopathic disorder caused by the loss of dopaminergic neurons in the substantia

nigra pars compacta (SNpc) and subsequent depletion of dopamine levels in the striatum (Chen and others 2005). Protection of the scant remaining dopaminergic neurons has been suggested as a therapeutic stratagem since the discovery of neuroprotective effects of glial cell line-derived neurotrophic factor (GDNF) on dopaminergic neurons *in vitro* (Lin and others 1993). GDNF exerts its effects by regulating cell survival and cell differentiation through PI3K/Akt and Ras/ERK pathways (Toth and others 2002). The potential neuroprotection and neurorestoration effects of GDNF have been examined in both rodent and non-human primate models of PD with positive effects shown in a variety of them (Eslamboli and others 2003; Kirik and others 2000; Pascual and others 2008). These encouraging results then prompted initial open-label clinical trials, which suggested continuous delivery of GDNF (or its relative, neurturin) by protein infusion or viral vector-mediated delivery was efficacious in advanced PD patients (Gill and others 2003; Marks and others 2008). However, such results were not replicated in double-blind, phase II clinical trials (Lang and others 2006; Marks and others 2010). At this time, the mechanism underlying the uneven success of GDNF in these trials is unclear (Broadstock and Yáñez-Muñoz 2012). Viral vector-mediated delivery offers stability of expression but, once administered, expression of the neurotrophic factor is often constitutive. Therefore, it is crucial that such expression is both safe and well-tolerated. The use of viral vectors allows transcriptional targeting, which may also be beneficial (Hioki and others 2007; Jakobsson and others 2003; Li and others 2010). Further trials are being considered to search for an effective, safe, and stable vector-based system to deliver GDNF (Bartus and others 2011; Richardson and others 2011).

Following on these investigations, we have assessed the efficacy of the novel IDLVs for therapy in a PD rodent model. We report that IDLVs can provide efficient, long-lived and transcriptionally targeted transduction of brain cells when injected ahead of striatal lesioning. While *hGDNF* gene expression was higher from IPLVs, transduction with IDLVs resulted in

equally efficient neuroprotection and long-term improvements of behavioral symptoms in 6-OHDA-lesioned rats. Lack of significant IDLV integration was confirmed in animals injected with vector following striatal lesioning. These results underscore the effectiveness of IDLVs in the CNS and the scope for low-dose, low-risk therapies based on these novel vectors.

Materials and Methods

Lentiviral vector production and titration

Concentrated stocks of the 2nd and 3rd generation lentiviral vectors, both IPLVs and IDLVs, were produced by calcium phosphate transfection into HEK-293T cells as previously described (Yáñez-Muñoz and others 2006). Lentiviral transfer plasmids used in this study were pRRLsc-CMVp-*eGFP*-W, pRRLsc-hGFAPp-*eGFP*-W, and pHR'-hGFAPp-*hGDNF*-W. All vectors were self-inactivating, contained a central polypurine tract/central termination sequence (cPPT/cTS) and Woodchuck hepatitis virus post-transcriptional regulatory element (WPRE), and were pseudotyped with the vesicular stomatitis virus G protein (VSV-G) envelope. Viral titers were quantified by either flow cytometry using a FACSCanto II (BD Biosciences, UK) or qPCR using a Rotogen Q (QIAgen, UK) as described (Yáñez-Muñoz and others 2006), or by p24 ELISA kit (SAIC, Frederick, Maryland, USA) following the manufacturer's instructions.

Animals

All animal experiments were performed in accordance with the UK Animals (Scientific Procedures) Act, 1986. Forty-five male Sprague-Dawley rats (Charles River, UK) weighing 250-300 g at the start of the study were housed 2-3 rats/cage. Animals were maintained in a standard 12-hour light/dark cycle with free access to food and water.

Stereotaxic injection

Animals were kept under isoflurane anesthesia (5% in 100% O_2 for induction and 2.5% in 100% O_2 for maintenance). The nose bar was set at -3.3 mm. All injections were made using a 20 µl Hamilton syringe held within an automated syringe pump (World Precision Instruments), and the injection rate was 0.5 µl/min.

6-OHDA lesioning and lentiviral vector injections for vector integration analysis

Thirty minutes prior to surgical procedures, animals were injected with a combined solution of pargyline (5 mg/kg, i.p) and desipramine (25 mg/kg, i.p). A single injection of 6-OHDA (12.5 µg in 2.5 µl of 0.9% saline and 0.02% ascorbic acid) was made into the median forebrain bundle (co-ordinates from Bregma: AP -2.8; ML +2.0; DV – 9.0 mm). Animals were then allowed to recover for two weeks. To assess the effectiveness of 6-OHDA lesioning, animals were habituated in 40 cm flat-bottomed hemispherical bowls for 15 min. Animals were then injected with apomorphine hydrochloride (Tocris, UK; 1 mg/kg, i.p, dissolved in sterile water). Rotational behavior was scored for 30 min post-injection. Animals displaying at least four net contraversive rotations per minute were deemed to have over 90% loss of striatal dopamine terminals (Hefti and others 1980).

Four days following apomorphine injection, under isofluorane-induced anesthesia, animals received a single 2.5 µl injection of either IDLV-CMVp-*eGFP* ($2x10^8$ eGFP vector particles/ml), IPLV-CMVp-*eGFP* ($2x10^8$ eGFP vector particles/ml) or DMEM (PAA, UK) into the left striatum (co-ordinates from Bregma: AP +1.0; DV -5.0; ML +2.8 mm). Groups of animals were as follows: 6-OHDA-lesioned IDLV (n = 5), 6-OHDA-lesioned IPLV (n = 4), non-lesioned IDLV (n = 3), non-lesioned IPLV (n = 3), and non-lesioned vehicle (n = 2). One week post-vector injection, animals were killed by exposure to a rising concentration of CO_2 followed by cervical dislocation. The striata were rapidly dissected into RNAlater for subsequent LAM-PCR.

Integration site analyses by 3'LTR-mediated LAM-PCR

3'LTR LAM-PCR was performed as previously described to determine the lentiviral vector integration sites (Schmidt and others 2007). In brief, 400-1100 ng of DNA per sample was used for linear PCR to pre-amplify 3' vector genome junctions. After double-strand synthesis,

restriction digestion (*Tsp*509I and *Hpy*CH4IV) and adapter ligation, two nested exponential PCRs were performed. LAM-PCR amplicons were prepared for sequencing by 454 technology (454/Roche system) as previously described (Paruzynski and others 2010). A final PCR step was set up to include 454 sequencing adaptors and sample-specific barcodes. After sequencing, the obtained sequences were trimmed and aligned to the rat genome (assembly rn4) by a semi-automated bioinformatical data mining pipeline as previously described (Arens and others 2012).

Lentiviral vector injections and 6-OHDA lesioning to test neuroprotective effects

Animals received a single injection of either IPLV-GFAPp-*hGDNF* (*n* = 10), IDLV-GFAPp-*hGDNF* (*n* = 10), IPLV-GFAPp-*eGFP* (*n* = 5) or IDLV-GFAPp-*eGFP* (*n* = 5) into two sites of the right striatum (5 µl/site; 10^9 viral DNA copies/ml or $2x10^4$ ng p24/ml). Stereotaxic co-ordinates from Bregma: (1) AP +1.8; ML -2.5; DV -5.0 mm; (2) AP 0.0; ML -3.5; DV -5.0 mm. Two weeks post-vector transduction, animals were injected with a combined solution of pargyline (5 mg/kg, i.p) and desipramine (25 mg/kg, i.p). Thirty minutes later, 6-OHDA (2.5 µg/µl in 0.9% sterile saline and 0.02% ascorbic acid) was injected into the same locations as vector administration, 2 µl/ site. Reagents were obtained from Sigma Aldrich, UK, unless stated otherwise.

Amphetamine-induced rotational behavior in hGDNF-treated animals

Rotational tests were performed from three weeks after 6-OHDA lesioning, once per month for a period of 4 months. Animals were acclimatized in 40 cm diameter bowls for 30 min prior to injection with amphetamine (Sigma, UK, 5 mg/kg, i.p, dissolved in sterile water). The rotations were assessed for 90 min post-injection as one whole head to tail revolution, with contralateral and ipsilateral rotations counted separately.

GDNF detection by ELISA

Animals were sacrificed by cervical dislocation as described above. The striata were isolated and frozen immediately in liquid nitrogen. Tissues were homogenized in complete lysis buffer (Roche, UK) followed by a centrifugation at 14000 *g*, 4^{o}C for 15 min. Levels of GDNF were determined by hGDNF ELISA kit (Promega, UK) following the manufacturer's instructions.

Immunohistochemistry

Rat brains were collected, fixed in ice-cold 4% PFA and maintained at 4^{o}C for 3 days. Coronal sections were sliced at 50 µm thickness on a vibratome (Campden Instruments, UK) following an incubation in 1% BSA blocking buffer for an hour. Rabbit anti-TH antibody (Cat AB152, 1:1000, Millipore, UK) was added to sections containing the SN, whilst either mouse anti-NeuN (Cat MAB377, 1:500, Millipore, UK), rabbit anti-GFAP (Cat Z0334, 1:500, DAKO, UK) or rabbit anti-Iba1 (Cat 019-19741, 1:500, WAKO, UK) antibody was added to striatal sections. Sections were maintained at 4^{o}C overnight then washed and incubated with either goat anti-mouse AlexaFluor555 (Cat A21424, 1:500, Invitrogen, UK) or goat anti-rabbit AlexaFluor555 (Cat A21428, 1:500, Invitrogen, UK) antibody for an hour, in the dark. After another three washes in 1X PBS, sections were incubated with 1 µg/ml DAPI for 15 min and subsequently washed in 1X PBS before being mounted onto SuperFrost slides.

Image capture

Brain sections were visualized under an inverted fluorescence Axio Observer D1 microscope. Images were captured with an AxioCam combined with AxioVision software. Equipment and software were from Carl Zeiss, UK.

Cell counts

Overlapping parts from each section containing the SN were captured and stitched automatically by AxioVision software to create a mosaic image of the section. The number of TH+ cells

within the SNpc (identified through Paxinos and Watson Rat Brain Map, 6th edition, 2007) on each section was counted manually using ImageJ software. Cell counts from approximately 30 SNpc-containing serial sections were averaged to obtain the total TH+ cell number per section of the SNpc in the corresponding brain hemisphere.

Measurement of eGFP intensity

After image capture, the area of the striatum on each section was subsequently identified according to the Paxinos and Watson Rat Brain Map (6th edition, 2007). The eGFP intensity within this area was quantified by AxioVision software and divided by the area to obtain the value of eGFP intensity, expressed as arbitrary units per μm^2. The values for approximately 60 striatal sections from each brain were averaged to obtain the value for the corresponding brain.

Statistical analysis

Using Prism 5 software (GraphPad, San Diego, California, USA), data were analyzed and shown as means ± S.E.M, with error bars representing the S.E.M. "*n*" refers to the number of animals per group. Comparisons of statistical significance were assessed by one- or two-way ANOVA followed by Bonferroni's *post-hoc* test or 2-tailed Student's *t*-test. Significant levels were set at $*p < 0.05$, $**p < 0.01$, $***p < 0.001$.

Results

Residual integration levels of IDLVs in intact and lesioned rat striata

We and others have demonstrated that IDLVs only integrate at residual levels in a variety of tissues, including the CNS (Chick and others 2012; Mátrai and others 2011; Yáñez-Muñoz and others 2006). To confirm that this is also the case in the 6-OHDA-lesioned rat brain we performed comparative large-scale lentiviral insertion site analysis by linear amplification-mediated PCR (LAM-PCR) followed by high-throughput sequencing (pyrosequencing). Animals were lesioned with 6-OHDA or mock-treated, and 18 days later injected in the right striata with IDLV or IPLV expressing *eGFP*. One week after vector injection, striata were harvested and analyzed for vector integration. As expected, there were considerably fewer integration sites for IDLVs than IPLVs (**Table 1**). Most interestingly, frequencies of integration events were broadly similar within vector types when comparing lesioned and non-lesioned striata. These data suggest that disease status had no effect on the overall integration frequency of lentiviral vectors. **Supp Table 1** details the integration sites of IDLVs in the present study.

Lentiviral vector-mediated eGFP expression in the striatum of 6-OHDA-lesioned rats

Animals were injected with IPLV- and IDLV-GFAPp-*eGFP* vectors, followed by 6-OHDA lesioning two weeks later. Brain tissue was harvested 5 months post vector injection. We firstly demonstrated successful transduction with widespread eGFP production within the striatum (**Figs. 1a,b**). Cell identification by morphology and marker expression indicated specific cell types were targeted, with mainly astrocytes being transduced; no significant microglia or neuron transduction was noticed (**Figs. 1c,d**). Levels of eGFP in groups treated with IDLVs were about 2-fold lower than in those receiving IPLVs (**Fig. 1e**). No *eGFP* expression in the non-injected hemisphere (**Fig. 2a**) or anterograde expression in the SNpr (**Fig. 2b**) was detected. Our data

suggest a modest, spatially restricted activation of both astrocytes and microglia in the area surrounding the injection site (**Figs. 2c,d**).

hGDNF neuroprotection on dopaminergic neurons in the SNpc of 6-OHDA-lesioned rats

GDNF is naturally secreted by glial cells (Lin and others 1993), and complications from neuronal transgene expression are possible (Jakobsson and Lundberg 2006). Following this rationale, we employed an astrocyte-specific promoter, the glial fibrillary acidic protein promoter (GFAPp), to drive lentivector-mediated *GDNF* expression in our neuroprotection experiments. Animals were injected with IPLV- or IDLV-GFAPp-*hGDNF* vectors, using *eGFP*-expressing vectors as controls, followed two weeks later by 6-OHDA lesioning. Levels of hGDNF (measured by ELISA 5 months post-injection) in ipsilateral striata of rats receiving *hGDNF* vectors were 60 to 250-fold higher than in contralateral striata or in *eGFP*-treated rats. We also observed a five-fold difference in hGDNF levels between IPLV- and IDLV-*hGDNF*-treated groups, higher in the former (**Fig. 3**).

We investigated the potential neuroprotective effects of hGDNF on dopaminergic neurons by estimating the loss of TH+ cells in the SNpc five months post vector injection and lesioning. Following a 10 µg striatal injection of 6-OHDA, a 50% reduction from normal levels of dopaminergic cell bodies was detected in the ipsilateral hemisphere of control (*eGFP*-treated) groups. The reduction was only 30% in *hGDNF*-treated animals, with no statistical difference between IPLVs and IDLVs despite the 5-fold difference in hGDNF levels (p =0.48, **Fig. 4a**). **Figs. 4b-d** show representative images of the SN with no damage in the contralateral hemisphere, 30% TH+ cell loss in the ipsilateral hemisphere of *hGDNF*-treated groups and 50% TH+ cell loss in the ipsilateral hemisphere of *eGFP*-treated groups, respectively. These data

indicate an effective neuroprotection by hGDNF on dopaminergic neurons regardless of lentiviral integration proficiency.

Behavioral recovery of hGDNF-treated rats

The vector-injected and 6-OHDA-lesioned animals were subjected to amphetamine-induced rotational tests performed monthly, starting from 3 weeks post-lesioning. Animals showed a normal weight gain with no difference between groups (p = 0.59, **Fig. 5a**). A time-dependent reduction in number of rotations was observed in all groups (**Fig. 5b**). However, an extensive recovery, with 98% reduction in rotational turns by the third test, was only seen in *hGDNF*-treated animals, regardless of vector integration-proficiency. In contrast, those injected with *eGFP* vectors presented only 66% reduction. Furthermore, we detected significant differences in rotational behavior between *eGFP*- and *hGDNF*-treated groups within tests, starting from the second test. By quantifying the number of rotations at 10 minute intervals, we noted that these differences occurred from minute 50 onwards (**Figs. 6a-d**). These results demonstrate that higher *hGDNF* expression resulting from IPLV administration (**Fig. 3a**) does not lead to any significant difference in the behavioral recovery compared to IDLVs (p = 0.36).

Discussion

Since we and others first reported safe and efficient *in vivo* transduction with IDLVs (Philippe and others 2006; Yáñez-Muñoz and others 2006), there has been scope for application to gene therapy for a major disease. Here we have investigated IDLV transduction for PD gene therapy in an animal model, in direct comparison with the commonly used IPLVs. Our data demonstrate that IDLVs injected ahead of striatal lesioning support long-lasting transduction of CNS cells for at least 5 months post-administration. We report a sustained therapeutic effect in this animal model following such IDLV-mediated neuroprotection, which was not significantly different to that of their integrating counterparts and persisted for the duration of the experiment.

Lentiviral vectors are an attractive system for gene therapy, with many positive features derived from their biology and extensive vector development, such as large transgene capacity of up to 8 kb, low immunogenicity (Mátrai and others 2010), enhanced cell-specific targeting through pseudotyping (Cannon and others 2011) and relatively simple production (Dull and others 1998). Moreover, they can transduce many cell types of the CNS (Jakobsson and others 2003), including dividing as well as non-dividing cells, with stable long-term expression of transgene(s) (Cockrell and Kafri 2007). Effective transgene expression can be obtained at low vector doses, 3-4 logs lower than AAVs, which have been widely used in gene therapy for PD treatment. Using lentiviral vectors, therefore, may be a significant advantage considering the potential of side-effects which may be associated with high vector doses (Bartus and others 2011; Drinkut and others 2012). However, a significant obstacle in the routine clinical use of current IPLVs is the potential for insertional mutagenesis and subsequent oncogenesis caused by integration of the viral genome into the host cell genome (Biasco and others 2012). This risk could be addressed by using IDLVs if the target cell population does not divide significantly (Banasik and McCray 2010; Wanisch and Yáñez-Muñoz 2009).

In the current work, we have assessed striatal integration of stereotaxically injected lentiviral vectors in normal rats or rats previously lesioned with 6-OHDA. Using LAM-PCR followed by pyrosequencing, we have only observed marginal integration levels of IDLVs, in agreement with previous analyses of IDLV integration *in vivo* (Chick and others 2012; Mátrai and others 2011; Yáñez-Muñoz and others 2006). Extending previous observations, we noticed that such residual integration did not change significantly in the presence of the striatal lesion.

Due to the lack of integration, transgene expression induced following IDLV administration can be reduced by cell division, though a similar disadvantage is well-known in the equally replication-deficient AAVs. In addition, although transcriptional targeting through the use of cell-type specific promoters may be beneficial (Hioki and others 2007; Jakobsson and others 2003; Li and others 2010), the GFAPp promoter may be less efficient in an episomal configuration, as observed with some promoters (Wanisch and Yáñez-Muñoz 2009). Astrocyte proliferation stimulated following CNS injury would therefore be predicted to result in less effective astrocytic *eGFP* or *hGDNF* expression following transduction with IDLV-GFAPp than IPLV-GFAPp. However, the stimulation of proliferation is temporary (Drinkut and others 2012) and rarely observed in the pathophysiology of PD (Mirza and others 2000). Indeed the results from this study indicate that proliferation and episomal expression were no major obstacles, with IDLV vectors driven by GFAPp expressing moderately lower levels of *eGFP* (2-fold) and *hGDNF* (5-fold) than their integrating counterparts. Moreover, high levels of *hGDNF* expression may be disadvantageous (Georgievska and others 2004). Using lentiviral vector-mediated intrastriatal delivery, these authors demonstrated that hGDNF levels above 700 pg/mg tissue weight caused a down-regulation of striatal TH levels and a significant reduction in mRNA level of this enzyme in the SN. Although the reductions might be restored 4-8 weeks later (Cohen and others 2011), it is unclear whether these changes may in turn affect striatal dopamine levels. The IDLVs here provided safe levels of hGDNF that were about 3-fold less than the reported over-

expression threshold. Importantly, the beneficial therapeutic effects of IDLV-*hGDNF* on survival of nigral dopaminergic cells were as efficient as those from IPLVs, which surpassed the 700 pg/mg threshold.

Numerous studies (Ciesielska and others 2011; Drinkut and others 2012; Jakobsson and others 2003; Richardson and others 2011) have previously reported that striatal transgene expression targeted to neurons resulted in transgene products in the SNpc/pr, the globus pallidus, and the subthalamic nucleus, in both lesioned and unlesioned hemispheres. This was possibly due to retrograde delivery from striatal dopaminergic nerve terminals to the cell bodies in the SNpc (Tomac and others 1995) and anterograde axonal transport from striatal neurons to the afferent regions via the indirect pathway, plus axonal sprouting between the two striatal hemispheres (Ciesielska and others 2011; Richardson and others 2011). These off-target effects may provide some advantages in GDNF application for PD treatment, but levels of GDNF transported indirectly to these afferent regions are unpredictable, particularly when higher vector doses or longer expression times are required (Bartus and others 2011; Drinkut and others 2012). It also remains unclear what the adequate level of GDNF required by these regions is, in order to provide therapeutic effects and simultaneously minimize side-effects (Georgievska and others 2004). In the light of the possible complications from neuronal transgene expression, we chose to target expression to astrocytes (Jakobsson and Lundberg 2006). Whilst neuronal axons can be several centimetres long, astrocytic protrusions rarely extend more than 20 μm from the cell body. Such a natural physical barrier may diminish off-target expression of transgene(s). In fact, the present study demonstrated astrocytic-*eGFP* expression targeted by IPLV- or IDLV-GFAPp vectors mainly in the injected striatum; a small proportion of cells in the white matter were transduced, presumably as a result of the backflow that occurs following withdrawal of the injection needle (Jakobsson and others 2003). Such an approach may therefore lead to maximal transgene expression in the required brain region, whilst preventing off-target effects resulting

from ectopic expression in afferent regions. Moreover, since astrocytes are the major source of GDNF upon brain injury and may be responsible for maintenance of GDNF levels in the SN of PD brains (Mogi and others 2001; Saavedra and others 2008), astrocytic-*hGDNF* expression by the lentiviral vector-GFAPp would be beneficial as demonstrated in this study.

One further advantage of lentiviral vectors is the minimal stimulation of the immune response that may occur following transgene delivery (Abordo-Adesida and others 2005; Mátrai and others 2010). Indeed, we only detected an elevated density of activated microglia and astrocytes surrounding the needle tract, which most likely reflects physical damage following injection of vectors and/or 6-OHDA rather than immune system activation following cell transduction (Batchelor and others 1999). This finding is consistent with previous studies (Drinkut and others 2012; Jakobsson and others 2003) regardless of whether lentiviral vectors or AAVs were used. In the current study the astrogliosis was prolonged up to 5 months, the end of the experiment, whereas Drinkut and colleagues reported that activated cells disappeared 3 months post-injection (Drinkut and others 2012). A possible explanation can be that in our study both vectors and 6-OHDA were administered into the same location, with concomitant doubling of physical trauma to the brain regions following repeated injections. As such, our approach may cause more physical damage than vector injection into the brain separated from intraperitoneal injection of MPTP in the previous study.

The neuroprotective effects of GDNF were also confirmed here through an improvement in amphetamine-induced rotational asymmetry of treated animals. Rats with a partial 6-OHDA lesion (less than 70% nigral dopaminergic cell loss) improve their rotational behavior over time, returning to nearly normal by about week 16 post-lesioning (Stanic and others 2003). This may be a consequence of regeneration of striatal dopaminergic terminals induced by GDNF or BDNF secreted from activated microglia in the injured striatum (Batchelor and others 1999). Such findings may explain the reduction in the number of rotations in all animal groups observed

here. However, only those animals injected with *hGDNF*-expressing vectors displayed an essentially complete recovery of behavior, which started from week 9 following vector injection. This recovery occurred regardless of vector integration proficiency.

In the present study, we chose to test a neuroprotection approach in which *hGDNF* lentivectors were administered prior to 6-OHDA lesioning. This strategy should be optimal for prevention of axonal retraction and subsequent neuronal death and indeed rendered a positive outcome. However, in PD patients the effects of neurotrophic factor therapy may also include neurorestoration of damaged neurons and neuroregeneration with new neurons in the injured regions. Therefore, further assessment of the effectiveness of IDLV-*hGDNF* expression for PD should include an experimental strategy in which 6-OHDA lesioning precedes the injection of therapeutic vector.

In summary, our study demonstrates IDLV-mediated neuroprotection in rats when intrastriatal *hGDNF* expression precedes 6-OHDA-lesioning. These data also show promoter-mediated cell-type specificity from IDLVs, with a focus on effective astrocytic transgene expression. We demonstrate both efficient delivery and long-lasting expression of a therapeutically relevant transgene by IDLVs at low dose. We also demonstrate lack of significant IDLV integration in this PD lesion model, supporting these safer vectors as potential tools in gene therapy for PD treatment, and by extension for other major diseases of the CNS. Our data warrant further exploration of IDLVs in PD-relevant models, in particular non-human primates, prior to considering clinical application. Demonstration of safety and efficacy in such models would strongly support the use of IDLVs in first-in-man studies.

Acknowledgments

The authors thank C. Lundberg (Wallenberg Neuroscience Center, Lund University, Sweden) for plasmid pHR'-hGFAPp-*hGDNF*-W. Steffanie Wiltcher assisted with the scoring of the behavioral experiment. This work received financial support from the 6th EU Framework Programme (CLINIGENE, grant agreement no. 18933), the 7th EU Framework Programme (NEUGENE, grant agreement no. 222925) and a studentship from Royal Holloway - University of London and University of Medicine and Pharmacy at Ho Chi Minh city, Vietnam. Author contributions: R.J.Y.-M. conceived and directed the project; R.J.Y.-M., M.B., M.Schm. and C.v.K. designed the experiments; N.-B.L.-N., M.B., M.Schl. and C.B. performed all experiments; all authors contributed to data analysis; N.-B.L.-N., M.B. and R.J.Y.-M. wrote the manuscript, with input from all authors.

Author Disclosure Statement

The authors declared no conflict of interest.

References

ABORDO-ADESIDA E, FOLLENZI A, BARCIA C, SCIASCIA S, *et al.* (2005). Stability of lentiviral vector-mediated transgene expression in the brain in the presence of systemic antivector immune responses. Hum Gene Ther 16, 741-51.

AIUTI A, BIASCO L, SCARAMUZZA S, FERRUA F, *et al.* (2013). Lentiviral hematopoietic stem cell gene therapy in patients with Wiskott-Aldrich syndrome. Science 341, 1233151.

APOLONIA L, WADDINGTON SN, FERNANDES C, WARD NJ, *et al.* (2007). Stable gene transfer to muscle using non-integrating lentiviral vectors. Mol Ther 15, 1947-54.

ARENS A, APPELT JU, BARTHOLOMAE C, GABRIEL R, *et al.* (2012). Bioinformatical Clonality Analysis of Next Generation Sequencing Derived Viral Vector Integration Sites. Hum Gene Ther Methods.

BANASIK MB, MCCRAY PB, JR. (2010). Integrase-defective lentiviral vectors: progress and applications. Gene therapy 17, 150-7.

BARTUS RT, BROWN L, WILSON A, KRUEGEL B, *et al.* (2011). Properly scaled and targeted AAV2-NRTN (neurturin) to the substantia nigra is safe, effective and causes no weight loss: support for nigral targeting in Parkinson's disease. Neurobiology of disease 44, 38-52.

BATCHELOR PE, LIBERATORE GT, WONG JY, PORRITT MJ, *et al.* (1999). Activated macrophages and microglia induce dopaminergic sprouting in the injured striatum and express brain-derived neurotrophic factor and glial cell line-derived neurotrophic factor. J Neurosci 19, 1708-16.

BIASCO L, BARICORDI C, AIUTI A. (2012). Retroviral integrations in gene therapy trials. Mol Ther 20, 709-16.

BIFFI A, BARTOLOMAE CC, CESANA D, CARTIER N, *et al.* (2011). Lentiviral vector common integration sites in preclinical models and a clinical trial reflect a benign integration bias and not oncogenic selection. Blood 117, 5332-9.

BJORKLUND A, KIRIK D, ROSENBLAD C, GEORGIEVSKA B, *et al.* (2000). Towards a neuroprotective gene therapy for Parkinson's disease: use of adenovirus, AAV and lentivirus vectors for gene transfer of GDNF to the nigrostriatal system in the rat Parkinson model. Brain research 886, 82-98.

BROADSTOCK M, YÁÑEZ-MUÑOZ RJ. (2012). Challenges for gene therapy of CNS disorders and implications for Parkinson's disease therapies. Hum Gene Ther 23, 340-3.

CANNON JR, SEW T, MONTERO L, BURTON EA, *et al.* (2011). Pseudotype-dependent lentiviral transduction of astrocytes or neurons in the rat substantia nigra. Experimental neurology 228, 41-52.

CHEN Q, HE Y, YANG K. (2005). Gene therapy for Parkinson's disease: progress and challenges. Current gene therapy 5, 71-80.

CHICK HE, NOWROUZI A, FRONZA R, MCDONALD RA, *et al.* (2012). Integrase-deficient lentiviral vectors mediate efficient gene transfer to human vascular smooth muscle cells with minimal genotoxic risk. Hum Gene Ther 23, 1247-57.

CIESIELSKA A, MITTERMEYER G, HADACZEK P, KELLS AP, *et al.* (2011). Anterograde axonal transport of AAV2-GDNF in rat basal ganglia. Mol Ther 19, 922-7.

COCKRELL AS, KAFRI T. (2007). Gene delivery by lentivirus vectors. Mol Biotechnol 36, 184-204.

COHEN AD, ZIGMOND MJ, SMITH AD. (2011). Effects of intrastriatal GDNF on the response of dopamine neurons to 6-hydroxydopamine: time course of protection and neurorestoration. Brain research 1370, 80-8.

CONDIOTTI R, GOLDENBERG D, GILADI H, SCHNITZER-PERLMAN T, *et al.* (2013). Transduction of Fetal Mice With a Feline Lentiviral Vector Induces Liver Tumors Which Exhibit an E2F Activation Signature. Mol Ther.

DRINKUT A, TERESHCHENKO Y, SCHULZ JB, BAHR M, *et al.* (2012). Efficient gene therapy for Parkinson's disease using astrocytes as hosts for localized neurotrophic factor delivery. Mol Ther 20, 534-43.

DULL T, ZUFFEREY R, KELLY M, MANDEL RJ, *et al.* (1998). A third-generation lentivirus vector with a conditional packaging system. J Virol 72, 8463-71.

ESLAMBOLI A, CUMMINGS RM, RIDLEY RM, BAKER HF, *et al.* (2003). Recombinant adeno-associated viral vector (rAAV) delivery of GDNF provides protection against 6-OHDA lesion in the common marmoset monkey (Callithrix jacchus). Experimental neurology 184, 536-48.

GEORGIEVSKA B, KIRIK D, BJORKLUND A. (2004). Overexpression of glial cell line-derived neurotrophic factor using a lentiviral vector induces time- and dose-dependent downregulation of tyrosine hydroxylase in the intact nigrostriatal dopamine system. The Journal of neuroscience : the official journal of the Society for Neuroscience 24, 6437-45.

GILL SS, PATEL NK, HOTTON GR, O'SULLIVAN K, *et al.* (2003). Direct brain infusion of glial cell line-derived neurotrophic factor in Parkinson disease. Nat Med 9, 589-95.

HACEIN-BEY-ABINA S, VON KALLE C, SCHMIDT M, LE DEIST F, *et al.* (2003). A serious adverse event after successful gene therapy for X-linked severe combined immunodeficiency. N Engl J Med 348, 255-6.

HEFTI F, MELAMED E, SAHAKIAN BJ, WURTMAN RJ. (1980). Circling behavior in rats with partial, unilateral nigro-striatal lesions: effect of amphetamine, apomorphine, and DOPA. Pharmacology, biochemistry, and behavior 12, 185-8.

HIOKI H, KAMEDA H, NAKAMURA H, OKUNOMIYA T, *et al.* (2007). Efficient gene transduction of neurons by lentivirus with enhanced neuron-specific promoters. Gene therapy 14, 872-82.

HUTSON TH, VERHAAGEN J, YÁÑEZ-MUÑOZ RJ, MOON LD. (2012). Corticospinal tract transduction: a comparison of seven adeno-associated viral vector serotypes and a non-integrating lentiviral vector. Gene Ther 19, 49-60.

JAKOBSSON J, ERICSON C, JANSSON M, BJORK E, *et al.* (2003). Targeted transgene expression in rat brain using lentiviral vectors. Journal of neuroscience research 73, 876-85.

JAKOBSSON J, LUNDBERG C. (2006). Lentiviral vectors for use in the central nervous system. Mol Ther 13, 484-93.

KIRIK D, ROSENBLAD C, BJORKLUND A. (2000). Preservation of a functional nigrostriatal dopamine pathway by GDNF in the intrastriatal 6-OHDA lesion model depends on the site of administration of the trophic factor. The European journal of neuroscience 12, 3871-82.

LANG AE, GILL S, PATEL NK, LOZANO A, *et al.* (2006). Randomized controlled trial of intraputamenal glial cell line-derived neurotrophic factor infusion in Parkinson disease. Annals of neurology 59, 459-66.

LI M, HUSIC N, LIN Y, CHRISTENSEN H, *et al.* (2010). Optimal promoter usage for lentiviral vector-mediated transduction of cultured central nervous system cells. Journal of neuroscience methods 189, 56-64.

LIN LF, DOHERTY DH, LILE JD, BEKTESH S, *et al.* (1993). GDNF: a glial cell line-derived neurotrophic factor for midbrain dopaminergic neurons. Science 260, 1130-2.

LYONS KE, PAHWA R. (2011). Diagnosis and initiation of treatment in Parkinson's disease. The International journal of neuroscience 121 Suppl 2, 27-36.

MARKS WJ, JR., BARTUS RT, SIFFERT J, DAVIS CS, *et al.* (2010). Gene delivery of AAV2-neurturin for Parkinson's disease: a double-blind, randomised, controlled trial. Lancet neurology 9, 1164-72.

MARKS WJ, JR., OSTREM JL, VERHAGEN L, STARR PA, *et al.* (2008). Safety and tolerability of intraputaminal delivery of CERE-120 (adeno-associated virus serotype 2-neurturin) to patients with idiopathic Parkinson's disease: an open-label, phase I trial. Lancet neurology 7, 400-8.

MÁTRAI J, CANTORE A, BARTHOLOMAE CC, ANNONI A, *et al.* (2011). Hepatocyte-targeted expression by integrase-defective lentiviral vectors induces antigen-specific tolerance in mice with low genotoxic risk. Hepatology 53, 1696-707.

MÁTRAI J, CHUAH MK, VANDENDRIESSCHE T. (2010). Recent advances in lentiviral vector development and applications. Mol Ther 18, 477-90.

MIRZA B, HADBERG H, THOMSEN P, MOOS T. (2000). The absence of reactive astrocytosis is indicative of a unique inflammatory process in Parkinson's disease. Neuroscience 95, 425-32.

MOGI M, TOGARI A, KONDO T, MIZUNO Y, *et al.* (2001). Glial cell line-derived neurotrophic factor in the substantia nigra from control and parkinsonian brains. Neuroscience letters 300, 179-81.

NOWROUZI A, CHEUNG WT, LI T, ZHANG X, *et al.* (2013). The fetal mouse is a sensitive genotoxicity model that exposes lentiviral-associated mutagenesis resulting in liver oncogenesis. Mol Ther 21, 324-37.

PARUZYNSKI A, ARENS A, GABRIEL R, BARTHOLOMAE CC, *et al.* (2010). Genome-wide high-throughput integrome analyses by nrLAM-PCR and next-generation sequencing. Nat Protoc 5, 1379-95.

PASCUAL A, HIDALGO-FIGUEROA M, PIRUAT JI, PINTADO CO, *et al.* (2008). Absolute requirement of GDNF for adult catecholaminergic neuron survival. Nature neuroscience 11, 755-61.

PELUFFO H, FOSTER E, AHMED SG, LAGO N, *et al.* (2013). Efficient gene expression from integration-deficient lentiviral vectors in the spinal cord. Gene Ther 20, 645-57.

PHILIPPE S, SARKIS C, BARKATS M, MAMMERI H, *et al.* (2006). Lentiviral vectors with a defective integrase allow efficient and sustained transgene expression in vitro and in vivo. Proc Natl Acad Sci U S A 103, 17684-9.

RAHIM AA, WONG AM, HOWE SJ, BUCKLEY SM, *et al.* (2009). Efficient gene delivery to the adult and fetal CNS using pseudotyped non-integrating lentiviral vectors. Gene Ther 16, 509-20.

RICHARDSON RM, KELLS AP, ROSENBLUTH KH, SALEGIO EA, *et al.* (2011). Interventional MRI-guided putaminal delivery of AAV2-GDNF for a planned clinical trial in Parkinson's disease. Mol Ther 19, 1048-57.

SAAVEDRA A, BALTAZAR G, DUARTE EP. (2008). Driving GDNF expression: the green and the red traffic lights. Progress in neurobiology 86, 186-215.

SCHMIDT M, SCHWARZWAELDER K, BARTHOLOMAE C, ZAOUI K, *et al.* (2007). High-resolution insertion-site analysis by linear amplification-mediated PCR (LAM-PCR). Nat Methods 4, 1051-7.

STANIC D, PARISH CL, ZHU WM, KRSTEW EV, *et al.* (2003). Changes in function and ultrastructure of striatal dopaminergic terminals that regenerate following partial lesions of the SNpc. J Neurochem 86, 329-43.

THEMIS M, WADDINGTON SN, SCHMIDT M, VON KALLE C, *et al.* (2005). Oncogenesis following delivery of a nonprimate lentiviral gene therapy vector to fetal and neonatal mice. Mol Ther 12, 763-71.

TOMAC A, WIDENFALK J, LIN LF, KOHNO T, *et al.* (1995). Retrograde axonal transport of glial cell line-derived neurotrophic factor in the adult nigrostriatal system suggests a trophic role in the adult. Proc Natl Acad Sci U S A 92, 8274-8.

TOTH G, YANG H, ANGUELOV RA, VETTRAINO J, *et al.* (2002). Gene transfer of glial cell-derived neurotrophic factor and cardiotrophin-1 protects PC12 cells from injury: involvement of the phosphatidylinositol 3-kinase and mitogen-activated protein kinase kinase pathways. Journal of neuroscience research 69, 622-32.

WANISCH K, YÁÑEZ-MUÑOZ RJ. (2009). Integration-deficient lentiviral vectors: a slow coming of age. Mol Ther 17, 1316-32.

YÁÑEZ-MUÑOZ RJ, BALAGGAN KS, MACNEIL A, HOWE SJ, *et al.* (2006). Effective gene therapy with nonintegrating lentiviral vectors. Nat Med 12, 348-353.

Figure legends

Figure 1. *eGFP* expression in rat striata. The right striata were injected with IPLV- or IDLV-GFAPp-eGFP two weeks prior to unilateral 6-OHDA lesioning at the same position of vector administration. Representative serial striatal sections from (**a**) IPLV- and (**b**) IDLV-eGFP injected animals show both vector injection site and area of vector spread. Representative high-magnification images from (**c**) IPLV- and (**d**) IDLV-eGFP-injected striata, respectively, are shown. Cell-type identification by morphology and marker expression indicated the majority of eGFP+ cells were astrocytes (GFAP+); no significant microglia (Iba1+) or neuron (NeuN+) transduction was observed. Nuclei were stained blue with DAPI; scale bar: 2000 µm (**a,b**), 100 µm (**c,d**) and 20 µm (insets in **c,d**). (**e**) eGFP levels evaluated 5 months post-vector injection showed a two-fold difference between IPLVs and IDLVs. Data were analyzed for statistical significance by 2-tailed Student t- test; error bars represent the S.E.M; $n = 3$ per group; $^{**}p < 0.01$.

Figure 2. Lack of anterograde eGFP transport and restricted glial activation. Following striatal injection of IDLV-GFAPp-*eGFP* and unilateral 6-OHDA lesioning at the same site, **(a)** no IDLV-*eGFP* expression in the non-injected left hemisphere or (**b**) anterograde eGFP transport from the striatum to the SNpr (co-stained in red for TH+ cells) was detected. Glial activation was analysed by GFAP+ or Iba1+ staining (in red), respectively. Arrows indicate activated (**c**) astrocytes and (**d**) microglia surrounding the IDLV injection site, with images on right side additionally displaying eGFP production pattern. Nuclei were stained blue with DAPI; scale bar: 2000 µm (**a**), 1000 µm (**c,d**) and 500 µm (**b**).

Figure 3. *hGDNF* overexpression in injected striata. Five months after vector transduction and 6-OHDA lesioning, rat striata were harvested. Levels of hGDNF measured by ELISA showed no differences in the contralateral hemispheres between groups. In contrast, the levels of hGDNF detected in the ipsilateral hemispheres of *hGDNF*-treated groups (n = 10) were significantly higher than in *eGFP*-treated groups (n = 4). There was also a significant difference between IPLV- and IDLV-*GDNF*-treated groups. Statistical analysis with one-way ANOVA and Bonferroni's *post-hoc* test. Error bars represent the S.E.M; **p<0.01, ***p<0.001.

Figure 4. Effect of *hGDNF* expression on survival of dopaminergic neurons in the SNpc. (**a**) Five months after vector transduction and 6-OHDA lesioning, counts of TH+ cells in the SNpc from contralateral and ipsilateral striata demonstrated similar cell survival in the contralateral SNpc of all groups and the loss of about 50% TH+ cells in the ipsilateral SNpc of *eGFP*-treated groups (n = 10). Animals receiving *hGDNF* showed enhanced cell survival, with 70% TH+ cells remaining in both IPLV- and IDLV-treated groups (n = 10). (**b-d**) Representative images of the SN with (**b**) no damage in the contralateral hemisphere; (**c**) 30% TH+ cell loss in the ipsilateral hemisphere of *hGDNF*-treated groups; and (**d**) 50% TH+ cell loss in the ipsilateral hemisphere of *eGFP*-treated groups. Red cells are TH+; scale bar = 500 µm. Statistical analysis with one-way ANOVA and Bonferroni's *post-hoc* test. Error bars represent the S.E.M; **p<0.01, ***p<0.001.

Figure 5. hGDNF-mediated improvement in amphetamine-induced rotational movement. (**a**) Time-scale of the experiment superimposed on a weight gain chart, with no statistical difference in weight between groups at each time point. (**b**) Following 30 min acclimation, animals were injected with amphetamine and net 360^{o} rotations were scored for 90 min. *hGDNF*-treated groups showed a significantly improved recovery of behavior starting from the

2^{nd} monthly test, with similar improvements regardless of vector integration proficiency. Data were analyzed for statistical significance by two-way ANOVA and Bonferroni's *post-hoc* test. Error bars represent the S.E.M; $n = 10$ per group; $*p<0.05$.

Figure 6. Timing of hGDNF-mediated improvement in rotational behavior in lesioned rats. (**a-d**) Following 30 min acclimation, animals were injected with amphetamine and net 360^{o} rotations were scored every 10 min for 90 min in monthly rotational tests. The improved behavior in *hGDNF*-treated groups noted from the 2^{nd} test is due to lower rotation numbers from min 50. Data were analyzed for statistical significance by two-way ANOVA and Bonferroni's *post-hoc* test. Error bars represent the S.E.M; $n = 10$ per group; $*p<0.05$.

Table 1: Residual integration of IDLVs is not affected by striatal lesion status

		Integration sites	
		Lesioned	Non-lesioned
Exactly mappable	IDLV	9	8
	IPLV	1023	494
Total	IDLV	18	8
	IPLV	1142	555

The following groups of animals were analyzed: lesioned IDLV (*n* = 5), lesioned IPLV (*n* = 4), non-lesioned IDLV (*n* = 3), non-lesioned IPLV (*n* = 3). LAM-PCR samples were subjected to high-throughput pyrosequencing. The raw sequence data were processed to determine possible integration sites. These were mapped onto the rat genome, with the majority being exactly mappable and few multiple hits. A total of 104601 sequence reads were obtained, distributed as follows: lesioned IDLV (38917), lesioned IPLV (38162), non-lesioned IDLV (15080), non-lesioned IPLV (12442).

Figure 1

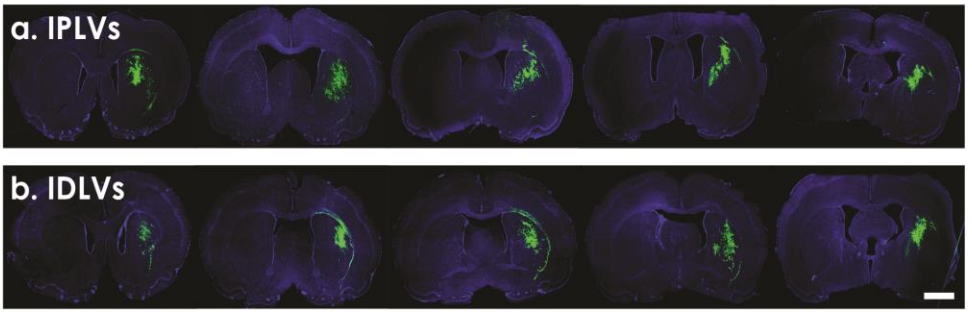
a. IPLVs
b. IDLVs

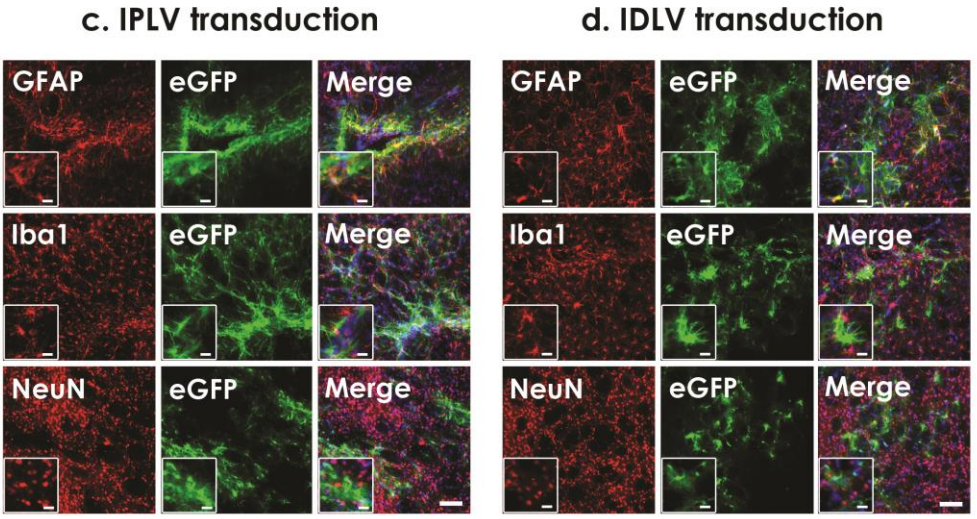
c. IPLV transduction
d. IDLV transduction
GFAP
eGFP
Merge
Iba1
eGFP
Merge
NeuN
eGFP
Merge
GFAP
eGFP
Merge
Iba1
eGFP
Merge
NeuN
eGFP
Merge

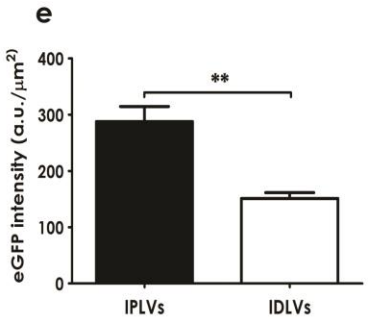
e
eGFP intensity (a.u./μm²)
400
300
200
100
0
**
IPLVs
IDLVs

Figure 2

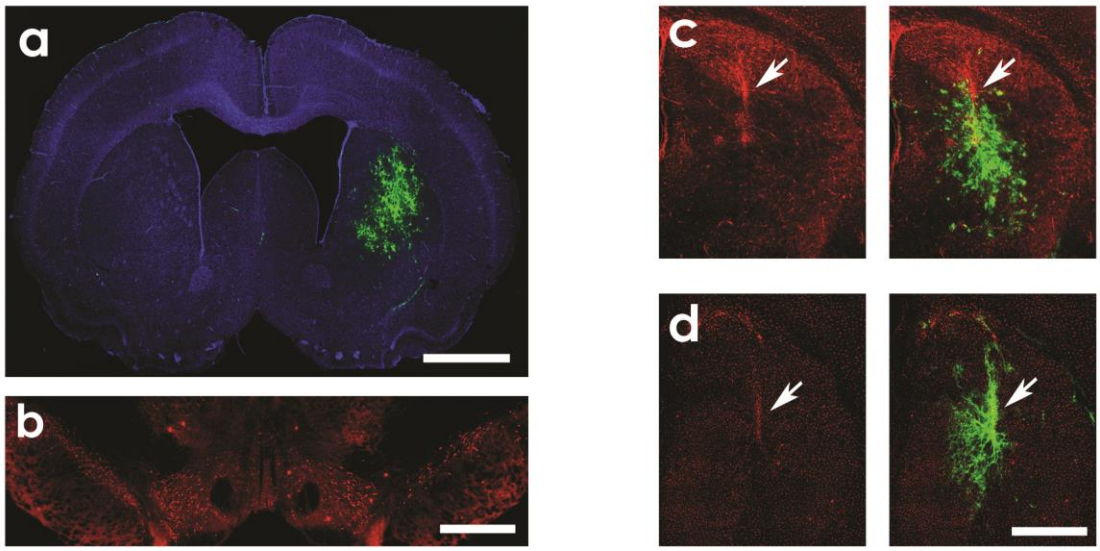

Figure 3

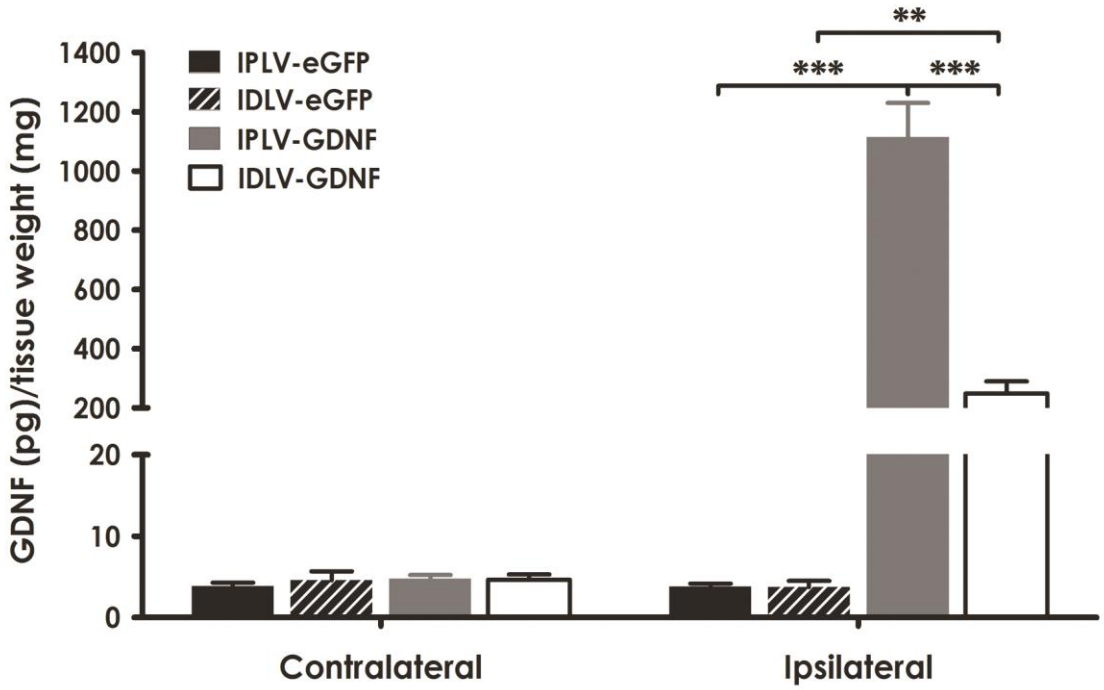
**
***
***
IPLV-eGFP
IDLV-eGFP
IPLV-GDNF
IDLV-GDNF
GDNF (pg)/tissue weight (mg)
1400
1200
1000
800
600
400
200
20
10
0
Contralateral
Ipsilateral

Figure 4

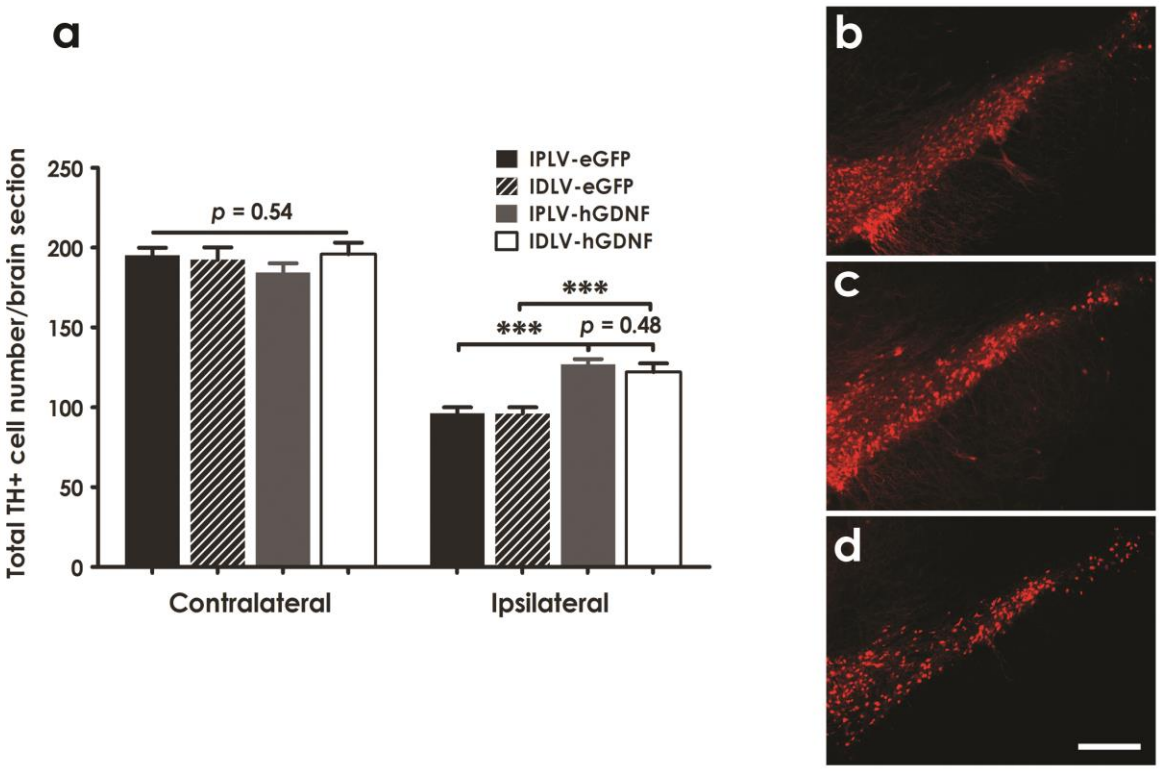
a
b
c
d
IPLV-eGFP
IDLV-eGFP
IPLV-hGDNF
IDLV-hGDNF
Total TH+ cell number/brain section
250
200
150
100
50
0
p = 0.54
***
***
p = 0.48
Contralateral
Ipsilateral

Figure 5

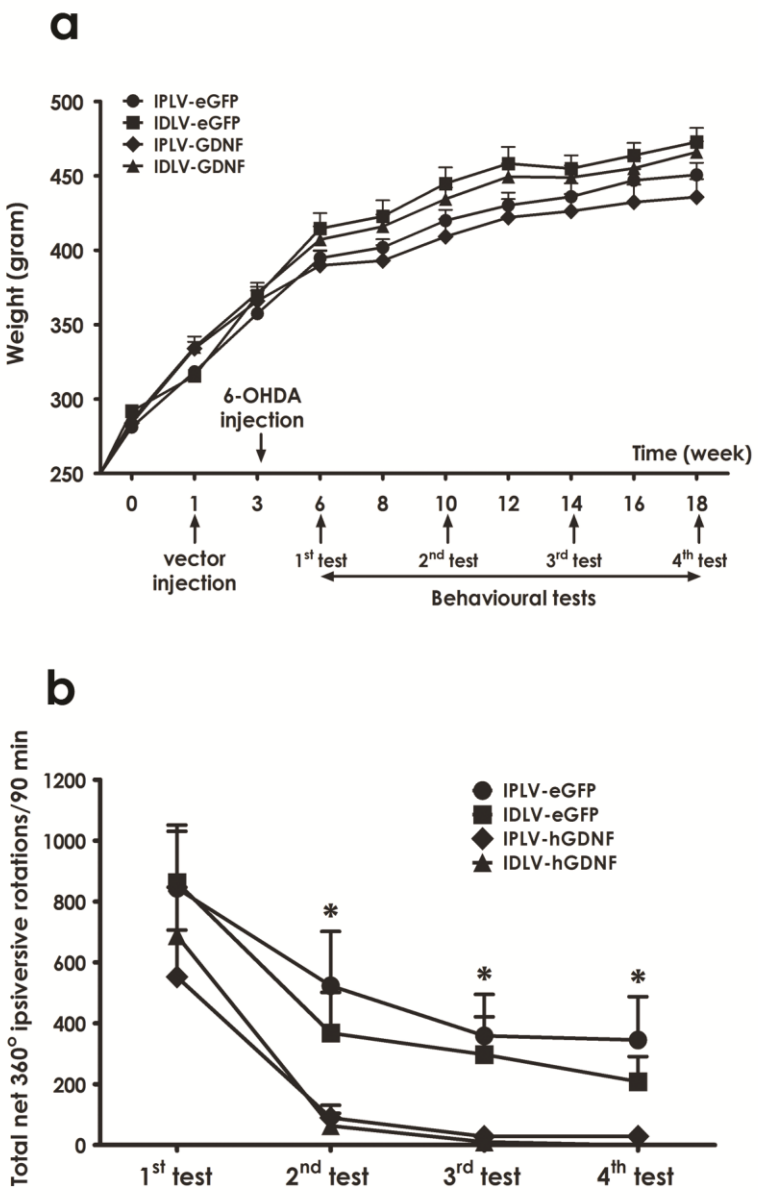
a
IPLV-eGFP
IDLV-eGFP
IPLV-GDNF
IDLV-GDNF
Weight (gram)
500
450
400
350
300
250
6-OHDA injection
Time (week)
0
1
3
6
8
10
12
14
16
18
vector injection
1st test
2nd test
3rd test
4th test
Behavioural tests
b
Total net 360° ipsiversive rotations/90 min
1200
1000
800
600
400
200
0
IPLV-eGFP
IDLV-eGFP
IPLV-hGDNF
IDLV-hGDNF
*
*
*
1st test
2nd test
3rd test
4th test

Figure 6

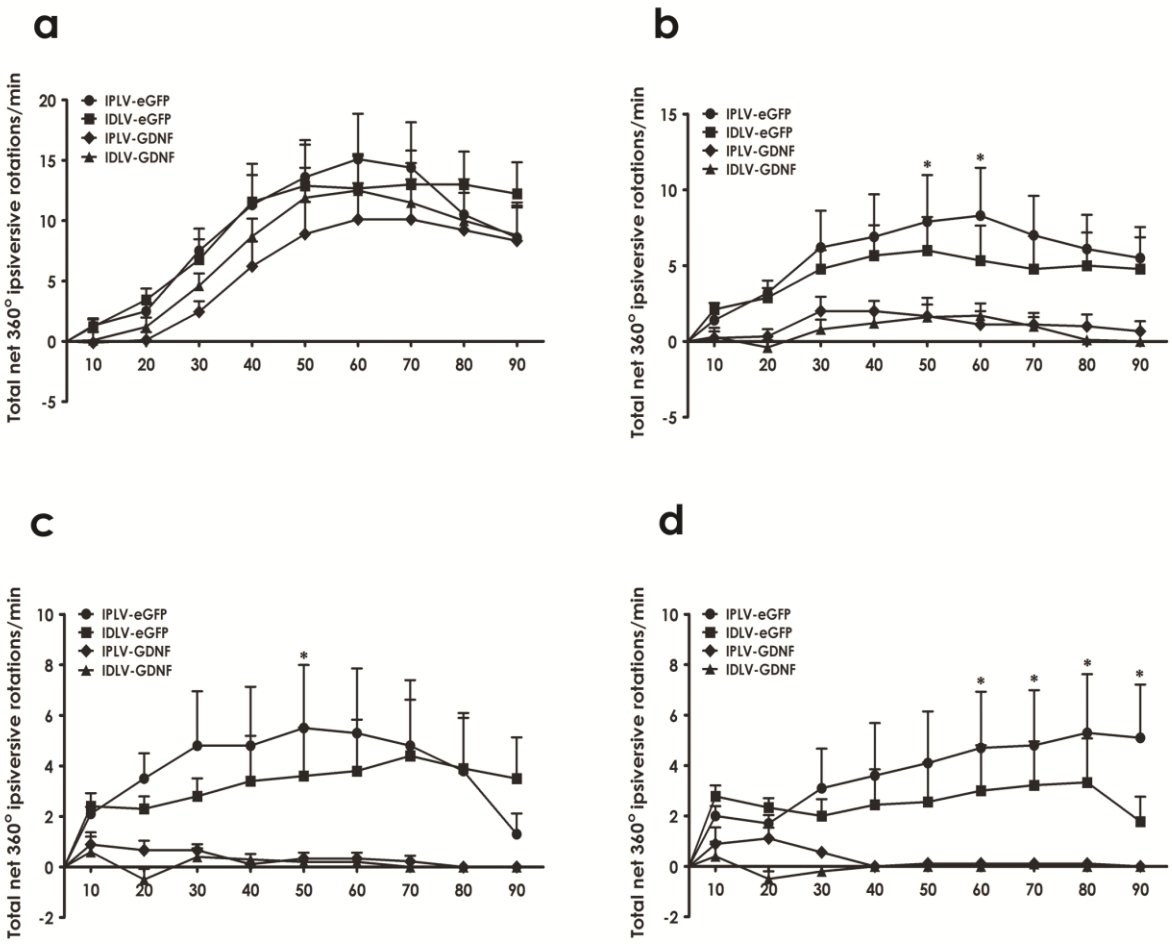
a
b
c
d
IPLV-eGFP
IDLV-eGFP
IPLV-GDNF
IDLV-GDNF
Total net 360° ipsiversive rotations/min
*

Supplementary Table 1. Integration events of IDLVs in rat striata

Status	Animal	Sample	DNA	Reads	Chr	Sequence Orientation	IL	Identity	Genomic Length	Upstream of TTS [bp]	In Gene Distance to TSS [bp]	Intron Exon	% in Gene	Downstream of Gene	RefSeq Gene	Gene length	Gene Orientation	RefSeq ID	Missing LTR Bases
Non-lesioned	14	15	877	1	19	+	49172372	99.3	142		665199	In5	62.288		Cdh13	1067948	+	NM_138889	10
Non-lesioned	14	15	877	2	2	+	77471363	100	128		51847	In2	35.366		Fam134b	146602	+	NM_001034912	1
Non-lesioned	14	15	877	1	2	+	77471406	100	85		51890	In2	35.395		Fam134b	146602	+	NM_001034912	20
Non-lesioned	15	21	697	27	10	-	40385868	98.48	66		53815	In25	96.6		Anxa6	55709	-	NM_024156	0
Non-lesioned	15	21	697	1	17	-	51216107	100	4-23(23)	11165					Trim27	12351	-	NM_001134974	0
Non-lesioned	16	27	1000	145	1	-	81102788	100	2-30(31)	79302					Cyp2s1	15023	-	NM_001107495	0
Non-lesioned	16	27	1000	1	16	+	88133136	100	4-23(24)	1806159					Slc10a2	243838	+	NM_017222	0
Non-lesioned	16	27	1000	5	6	-	47958552	100	81		67188	In16	94.775		Tpo	70892	-	NM_019353	0
Lesioned	6	51	397	3	8	-	69935674	100	3-22(24)		673	In1	4.868		Oaz2	13824	+	NM_001109899	0
Lesioned	7	57	535	1	16	+	20336721	96.84	96					71149	MGC72612	13960	+	NM_001009538	0
Lesioned	7	57	535	2	16	-	79570945	95	20		8691	Ex3	87.886		Cln8	9889	-	NM_001007686	0
Lesioned	7	57	535	1	17	+	35793267	99.65	286	275621					Cdyl	227392	-	NM_001014145	0
Lesioned	7	57	535	1	17	+	69041211	100	20		82169	In2	14.027		Ryr2	585775	+	NM_032078	0
Lesioned	7	57	535	1	3	-	56124081	100	20					19972	Chn1	42613	-	NM_032083	0
Lesioned	7	57	535	1	4	+	114228958	100	92		85027	In1	10.668		Lrrtm4	797018	+	NM_001134746	0
Lesioned	7	57	535	1	23	-	79829941	100	3-25(35)	382941					Mageb18	2253	-	NM_001044246	0
Lesioned	8	63	904	2032	2	-	220111914	98.57	2-281(281)		4653	In4	29.554		Mettl14	15744	-	NM_001106470	0

Chr, Chromosome; IL, Integration Locus; TSS Transcription start site